Galaxies or Asteroids? – 12 μm Sources in 9 QSO Fields Near the Ecliptic

A. C. Quillen[1,2]

ABSTRACT

We consider 9 fields of low ecliptic latitude observed at 12μm centered on QSOs. In these fields we detect 7 additional background sources at the level of 0.4-4mJy in 70 square arcminutes. 4 of these sources correspond to galaxies seen in the Digitized Sky Survey. 3 of these sources are not observed in this survey. The 4 sources with optical counterparts are low redshift objects with low infrared to optical flux ratios and so low inferred infrared luminosities $L_{FIR} \lesssim 10^9 L_\odot$. Statistical arguments suggest that the unidentified sources are more likely to be distant $L_{FIR} > 10^{10} L_\odot$ starbursting galaxies, rather than asteroids or late-type stars.

2 of our QSO fields are likely to have starbursting galaxies at moderately high redshift near the QSO (in angular scale). Since the lensing optical depth towards these QSOs is expected to peak at moderate redshift there is some possibility that these galaxies are in clusters that lense the QSOs. If none of our sources are asteroids then the number of small (km) sized main belt asteroids cannot be larger than 500,000 per absolute magnitude bin.

Subject headings: galaxies: evolution — galaxies: kinematics and dynamics — galaxies: spiral

1. Introduction

The ISO satellite (Kessler et al. 1996) is orders of magnitude more sensitive than IRAS at shorter IR wavelengths ($< 20\mu$m). Based on the local universe IR luminosity function (e.g. Saunders et al. 1990, Rieke & Lebofsky 1986) inferred by IRAS observations, it has been possible to make predictions for number counts of objects in the mid-far IR wavelength ranges at levels fainter than observed by IRAS. Number counts at the 1mJy level in the mid IR are expected to include both normal galaxies at moderate redshift ($z \sim 0.1$) as well as starbursts that could be detected out to $z \sim 1$ (e.g. Franceschini et al. 1994, Lonsdale et al. 1990, Oliver et al. 1997).

[1]University of Arizona, Steward Observatory, Tucson, AZ 85721

[2]E-mail: aquillen@as.arizona.edu

In this paper we consider background source counts in 9 QSO fields imaged at 12μm with ISOCAM. The area of sky covered is larger than the ISO Hubble Deep Field survey (Serjeant et al. 1997) but smaller than that being carried out by Cezarsky et al. 1997 at 25μm. Our fields are found in the ecliptic and so can also be used to place limits on the number of km sized asteroids in the Main Asteroid Belt. The association with QSOs also places crude limits on magnitude bias for these QSOs.

2. Observations

Images of 9 fields centered on QSOs using the LW10 filter ($8.6 - 14.4\mu$m) were taken with ISOCAM (Cesarsky et al. 1996) (a 32×32 array on the ISO satellite(Kessler et al. 1996) in the imaging mode with 6.0" per pixel. Each field was observed for a total of 114 exposures each 5.04s long, taken in a 3×3 raster on the sky that offset by 18" so that each of the nine sky positions were observed for a total of ~ 50 seconds with some additional time spent on the first position. The total integration time per field was 9.5 minutes. The dates and times of the observations are listed in Table 1.

Of these 114 exposures we discarded the first 30 because the array had not yet stabilized. After this time based on the subsequent flat level of the sky we judged the array to be stabilized. Cosmic ray glitches were removed using the 'MM' multi-resolution spatial and temporal routine in the CAM Interactive Analysis (CIA) package ([3] Because of the long exposures and long total integration time, low frequency noise was observed in each pixel as a function of time in the data after cosmic ray removal. To remove the low frequency noise we then removed third order polynomials from each pixel as a function of time. Following this procedure, flat fields were constructed from the images themselves by fitting a smooth function that varies with time to the entire data cube. The final mosaic was constructed from the nine mosaic positions with a least-squares fit to each pixel in the images after shifting them according to the position observed. The final images are shown in Figure 1.

We calibrated the final images by scaling the sky value back to the original value of the cmos ISO Automatic Analysis product which is estimated to be accurate within $\pm 30\%$ (Cesarsky et al. 1996). Since the images used were observed after stabilization had taken place this calibration should be accurate to the level specified. The resulting images have a pixel to pixel standard deviation of $\sim 30\mu$Jy per $6''$ pixel in the central 25×25 pixels. By removing some of the low frequency noise from the images we improved the pixel to pixel standard deviation by a factor of 1/5 from the cmos Automatic Analysis product.

In the center of the final images all the quasars are detected at the level of a few mJy. Because

[3]CAM Interactive Analysis is a joint development by the ESA astrophysics division and the ISOCAM consortium led by the ISOCAM PI, C. Ceśarsky, Direction des Sciences de la Matieère, C. E. A. , France

of the pointing performance of ISO (absolute pointing error less than a few arcsec, Kessler et al. 1996) we are confident that the central sources are indeed at the position of the QSOs.

7 additional sources (besides the QSOs) were detected in these images. We estimate that we are complete down to the 0.3mJy level. These sources were seen in different pixel locations in the various frames comprising the raster so we are confident that these sources are not spurious detections due to cosmic rays. Fluxes of these 7 sources are listed in Table 2.

Digitized Sky Survey images of the QSO field are shown in Figure 2 with identified sources marked. Of the 7 sources detected 4 are galaxies resolved in the sky survey images. We estimate V band magnitudes and magnitude limits, also listed in Table 2. from the Sky Survey images by scaling from the brightness of the central QSO. Approximate coordinate positions of the 7 sources are listed in Table 3. We judge these coordinate position to be accurate to $\pm 6''$, the pixel size of our 12μm images.

2.1. Number Density Estimates

The very edge of our field has a higher level of noise than the central region because of the effective integration time is only 1/9-1/3 as long as in the central field. We therefore included only the central 28 pixels in each image in our total effective area covered. The resulting area is 7.84 square arcminutes per QSO field with a total of 70 square arcminutes covered in our 9 fields. For the four identified galaxies sources we convert this to a number density of 100 – 300 distant galaxies per square degree at a limiting flux level of 0.5mJy (including Poisson statistical errors). For the 3 unidentified sources a similar 150 objects per square degree is estimated. Including all 7 sources we estimate a total of 300 - 500 objects per square degree.

3. Distant Galaxies

In Table 2 for comparison with other IRAS samples we have computed L_{IR}/L_{opt}. We estimate F_{opt} using νF_ν at (0.55μm or V band) which is within 10% of that estimated at estimated at 0.44μm for typical galaxy colors ($B - V \sim 0.5$). We estimate F_{IR} as νF_ν at 60μm using a conversion of $F_{\nu(60\mu rmm}/F_{\nu(12\mu\mathrm{m}} = 16$ based on the mean value of the IRAS bright galaxy sample (Soifer et al. 1989). This value of L_{IR} is approximately equal to the parameter L_{FIR} of Helou et al. 1988 based on the 60 and 100μm flux for a galaxy with a mean $F_{60\mu\mathrm{m}}/F_{100\mu\mathrm{m}} = 0.5$. For field galaxies no correlation between L_{IR} and $F_{60\mu\mathrm{m}}/F_{25\mu\mathrm{m}}$ was observed (Rieke & Lebofsky 1986) however there could be correlation between $F_{60\mu\mathrm{m}}/F_{12\mu\mathrm{m}}$ and L_{IR} because of the differing contributions of cirrus and star forming regions to the IR emission (Helou 1986) in quiescent and starbursting galaxies.

From Table 2 we can see that for the 4 galaxies with bright optical counterparts,

$\log(L_{IR}/L_{opt}) < 0.0$. Based on the correlation between L_{IR}/L_{opt} with L_{IR} (Soifer et al. 1989) this suggests that these galaxies are low luminosity $L_{IR} \sim 10^9 L_\odot$ galaxies (with $z < 0.1$). On the other hand the limiting flux ratios of the 3 12μm sources without optical counter parts are high enough that if they are galaxies they would have high IR luminosities $L_{IR} > 10^{10} L_\odot$ and therefore would be more distant ($z \sim 1$). If these sources are faint galaxies they should be visible in optical images deeper than the digitized sky survey images.

If all 7 of our 12μm sources are galaxies then our total number density is somewhat higher (a factor of 2-4 higher) than predicted by Franceschini et al. 1991 though within small number statistics our number density is similar to that predicted by Rieke et al. 1997. However the optical to IR color ratios differ from those predicted by these models for the 4 sources with optical counterparts. Using the local universe luminosity function of Saunders et al. 1990 and the distribution of $F_{12\mu\mathrm{m}}/F_{60\mu\mathrm{m}}$ from Soifer et al. 1989 we find that for sources at a limiting flux of 0.4mJy the mean luminosity is $L_{IR} \sim 10^{10} L_\odot$ and is larger than we infer from the optical to 12μm colors for the 4 sources with optical counter parts. However this discrepancy could be alleviated if there is a dependence of $F_{12\mu\mathrm{m}}/F_{60\mu\mathrm{m}}$ on L_{IR}, which is not unexpected if the emission from low luminosity galaxies is dominated by cirrus emission (Helou 1986).

If the 3 objects without counterparts are starbursting galaxies then as shown by Oliver et al. 1997, Mann et al. 1997 and Rowan-Robinson et al. 1997 cosmological models with evolution are required to explain the number counts. This is not unexpected based on the large number of high redshift starbursting galaxies observed in the Hubble Deep Field.

3.1. Magnitude or lensing bias and the possibility of association with with QSO

It is unlikely that any of our sources are at the QSO redshift since they are close in flux level to the QSO itself and such bright implied galaxies luminosities in the QSO environment are unlikely. The QSO's redshifts are $z = 1.5 - 2$ so that the lensing optical depth towards them peaks at about $z = 1$. This makes it unlikely that a lensing cluster at low redshift is responsible for both brightening the QSO and containing a galaxy detectable at 12μm. Spiral galaxies, being much more numerous and brighter in the mid-IR than ellipticals are more likely to be detected at 12μm and are unlikely to be in clusters. However it is possible that the 3 sources without optical counterparts are starbursting galaxies and are part of a cluster which could be lensing the QSOs.

4. Other Possibilities for the 3 Sources Without Optical Counterparts

4.1. The possibility of Galactic sources or M stars

Our fields are all at high galactic latitudes, greater than 55° from the galactic plane except for POX 42 which is at a galactic latitude of 42°. At these high galactic latitudes, most galactic

sources are too scarce to be observed at the number density that we observe them at the 0.5 mJy level at 12μm.

Here we consider the possibility that we could be detecting late M stars which are quite numerous. Using absolute V magnitudes from Leggett 1992 and V-[12] colors from Kenyon & Hartmann 1995 we estimate that an M0, M4 star would be detected in 12μm at the 0.5 mJy level to a distance of only 300 and 50 pc respectively. Summing the entire luminosity function (M0-M8) of Gould et al. 1996 over the volume limit given by the 0.5 mJy 12μm detection limit gives a total of ~ 20 sources expected per degree which is insufficient in number for us to expect the 3 sources we see in 70 square arcminutes. We therefore find that it is very unlikely that our 3 unidentified sources are late-type stars. We have not used the optical to 12μm color limits placed from the digitized sky survey because nearby stars could have moved since the sky survey images were observed.

According to the models of Burrows et al. 1997 a 1 Gyr old brown dwarf with a mass of 40 Jupiter masses would only be seen at a level of 0.5 mJy at a distance of 14 pc. A rather high total number density of 700 bright brown dwarfs per pc^3 would be required so that we could detect them in our images. It's very unlikely that our unidentified objects are brown dwarfs.

4.2. The possibility of asteroids

All of our fields are at low ecliptic latitude; within 10° of the ecliptic except POX 42 (at 18°) and 0059-2735 (at 27°) from the ecliptic. Here we consider the likelihood of detecting Main Belt asteroids.

None of our unidentified objects are numbered asteroids listed currently in the database provided by Minor Planet Center (operated at the Smithsonian Astrophysical Observatory, under the auspices of Commission 20 of the International Astronomical Union). Asteroids with known orbit elements, numbering about 35000, (The Asteroid Orbital Elements Database of Lowell Observatory) are only complete to about $H = 13$ absolute magnitude (where the absolute magnitude is computed at 1AU from both the observe and the sun in V band, Kuiper et al. 1958), and would be much brighter than 1mJy at 12μm if they were in the Main Belt (less than 4 AU from the sun).

We therefore must consider deeper asteroid surveys. As part of the Spacewatch Survey (Gehrels 1991), Jedicke & Metcalfe 1997 have completed a deep ($V < 21$) survey of the Main Asteroid Belt Jedicke & Metcalfe 1997 which is complete to $H \sim 17$. These authors find approximately 50000 asteroids per absolute magnitude bin in each of 3 regions. Their inner, mid and outer regions are centered at 2.25,2.75 and 3.25 AU respectively from the sun and are 0.5 AU wide. Using the standard thermal model, and a bond emissivity of 0.1, we estimate that asteroids of H =19,18, and 17 (having sizes of $\sim$ 0.8,1.3, and 2.0 km) would be detected at opposition at the 1mJy level in 12μm in the inner, mid and outer regions respectively. Jedicke & Metcalfe

1997 found that the numbers of asteroids does not depend strongly on the absolute magnitude for $15 < H < 17$. Using the number of asteroids measured at H=17 mag in their last complete magnitude bin and summing over the 3 regions we compute a total of 20 objects per square degree would be detected within 10° of the ecliptic at 12μm at the 1mJy level from the Main Belt (distributing the asteroids evenly within 10° of the ecliptic). It is therefore unlikely that all 3 of our sources are asteroids.

5. Discussion

We find that it most likely that our 7 additional sources are distant galaxies. The estimated number densisty of objects is somewhat higher than predicted from the local IRAS derived luminosity functions, however with additional star formation at high redshift our three sources with no bright optical counterparts are likely to be distant starbursting galaxies. The 4 sources with couterparts are only predicted with the local IRAS luminosity function if the 12μm flux is relatively high in low L_{IR} galaxies compared to starbursting galaxies, which is not unexpected since these galaxies should be dominated by emission from cirrus at 12 μm.

2 of our QSO fields (the ones that have 12μm sources with no bright optical counterparts) are likely to have starbursting galaxies at moderately high redshift near the QSO (in angular scale). Since the lensing optical depth towards these QSOs is expected to peak at $z \sim 1$ there is some possibility that these galaxies are in clusters that lense the QSOs. If none of our sources are asteroids then the number of small (km) sized main belt asteroids cannot be larger than 500,000 per absolute magnitude bin.

The Infrared Space Observatory (ISO) is an ESA project funded by ESA Member States (especially the PI countries: France, Germany, The Netherlands, and the United Kingdom with the participation of ISAS and NASA). We thank D. van Buren, M. Seh, K. Ganga, R. Hurt, L. Hermans and the ISO team at IPAC for help with the data reduction of the ISOCAM images.

I thank M. Sykes for his code that predicts 12μm fluxes of asteroids, and teaching me alot about about asteroids. We acknowledge helpful discussions and correspondence with R. Jedicke, M. Rieke, G. Rieke, P. Hall, D. Hines, R. Kennicutt, P. Massey, I. Hook, A. Gould, M. Sykes, C. Neese, T. Fleming, M. Hanson, R. Hurt, and K. Luhman. We also acknowledge support from NSF grant AST-9529190 and NASA project no. NAG-53359.

Figure 2 and Table 2 made use of the Digitized Sky Survey. The Digitized Sky Surveys were produced at the Space Telescope Science Institute under U.S. Government grant NAG W-2166. The images of these surveys are based on photographic data obtained using the Oschin Schmidt

Telescope on Palomar Mountain and the UK Schmidt Telescope. The plates were processed into the present compressed digital form with the permission of these institutions. The National Geographic Society - Palomar Observatory Sky Atlas (POSS-I) was made by the California Institute of Technology with grants from the National Geographic Society. The Second Palomar Observatory Sky Survey (POSS-II) was made by the California Institute of Technology with funds from the National Science Foundation, the National Geographic Society, the Sloan Foundation, the Samuel Oschin Foundation, and the Eastman Kodak Corporation. The Oschin Schmidt Telescope is operated by the California Institute of Technology and Palomar Observatory. The UK Schmidt Telescope was operated by the Royal Observatory Edinburgh, with funding from the UK Science and Engineering Research Council (later the UK Particle Physics and Astronomy Research Council), until 1988 June, and thereafter by the Anglo-Australian Observatory. The blue plates of the southern Sky Atlas and its Equatorial Extension (together known as the SERC-J), as well as the Equatorial Red (ER), and the Second Epoch [red] Survey (SES) were all taken with the UK Schmidt.

The research and computing needed to generate The Asteroid Orbital Elements Database were funded principally by NASA grant NAGW-1470, and in part by the Lowell Observatory endowment. This database is created and made available by T. Bowell.

REFERENCES

Bothun, G. D., Lonsdale, J. C., & Rice, W. 1989, ApJ, 341, 129

Burrows et al. 1997, ApJ, in press

Cezarsky, et al. in preparation

Cesarsky, C. J. et al. 1996, A&A, 315, L32

Franceschini, A., de Zotti, G., Toffolatti, L., Mazzei, P., Danese, L. 1991, A&AS, 89, 285

Franceschini, A., Mazzei, P., & de Zotti, G. 1994, ApJ, 427, 140

Gehrels, T. 1991, Space Science Review, 58, 347

Goldshmidt, P. et al. 1997, MNRAS, in press

Gould, A., Bahcall, J. N., & Flynn, C. 1996, ApJ, 465, 759

Helou, G., 1986, ApJ, 311, L33

Helou et al. 1988 Helou, G., Khan, I. R., Malek, L., & Boehmen, L. 1988, ApJS, 68, 151

Jedicke, R., & Metcalfe, T. S. 1997, submitted to Icarus

Kenyon, S. J., & Hartmann, L. 1995, ApJS, 101, 117

Kessler, M. F., Steinz, J. A., Anderegg, M. E., Clavel, J., Drechsel, G., Estaria, P., Faelker, J., Riedinger, J. R., Robson, A., Taylor, B. G., Ximnez de Ferrn, S. 1996, A&A, 315, L27

Kuiper, G. P., Fujita, Y., Gehrels, T., Groeneveld, I., Kent, J., van Biesbroeck, G., van Houten, C. J. 1958, ApJS, 32, 289

Leggett, S. K. 1992, ApJS, 82, 351

Lonsdale, C. J., Hacking, P. B., Conrow, T. P. 1990, ApJ358, 60

Mann, R. G. et al. 1997, MNRAS, in press

Oliver, S. J. et al. 1997, MNRAS, in press

Rieke, G. H., Young, E. T. Gautier, T. N. private communication

Rieke, G. H. Lebofsky, M. J. 1986, 304, 326

Rowan-Robinson , M. et al. 1997, MNRAS, in press

Saunders, W., Rowan-Robinson, M., Lawrence, A., Efstathiou, G., Kaiser, N., Ellis, R. S.,&, Frenk, C. S. 1990, MNRAS, 242, 318

Serjeant, S. et al. 1997, MNRAS, in press

Soifer, B. T., Boehmer, L., Neugebauer, G., Sanders, D. B. 1989, AJ, 98, 766

Soifer, B. T., Sanders, D. B., Madore, B. F., Neugebauer, G., Danielson, G. E., Elias, J. H., Lonsdale, J. C., Rice, W. L. 1987, ApJ, 320, 238

Table 1. Dates and Times of Observations

QSO Field	Date (UT)	Start Time	End Time
POX 42	28/07/96	05:43:34	05:53:31
UM 275	12/12/96	21:48:52	21:59:11
UM 208	06/12/96	19:51:25	20:01:49
0059-2735	30/11/96	03:59:32	04:09:53
1246-0542	28/07/96	06:52:36	07:03:01
UM 288	12/12/96	18:31:34	18:41:48
1309-0536	30/07/96	18:28:34	18:38:38
1331-0108	03/08/96	02:10:58	02:21:04

NOTES.– Dates are given as day/month/year.

Table 2. Source Fluxes and Offsets

Source[a]	QSO Field	Offset $x('')^b$	Offset $y('')^b$	$F_{12\mu m}$	V (mag)[c]	log F_{IR}/F^e_{opt}
1	POX 42	87.6	21.5	1.01 ± 0.12	18.1	-0.18
2	UM 275	29.1	-84.7	3.77 ± 0.18	>20.3	> 1.3
3	UM 275	-84.0	-10.1	0.48 ± 0.11	18.1	-0.53
4	UM 275	37.3	55.2	0.41 ± 0.10	>20.3	> 0.3
5	UM 208	32.4	-23.1	0.61 ± 0.10	16.1	-1.16
6	UM 208	-20.0	-84.6	0.49 ± 0.10	>20.5	> 0.5
7	0059-2735	43.9	-55.3	0.77 ± 0.10	16.8	-0.82

NOTES.– [a] We assign numbers to the detected sources. [b] Positions of source from the QSO where a positive x,y offset is to the west, north of the QSO respectively. Positions are accurate to $\pm 6''$. [c] V mag estimated from the Digitized Sky Survey images (see Figure 2) by scaling from the QSO V band magnitude. Values preceded with > are detection limits for sources that were not detected in the Digitized Sky Survey. [d] Flux ratio or limit from the Digitized sky survey? [e] See text.

Table 3. Astrometry of Sources

Source	RA(1950)	DEC(1950)
1	11:58:05.8	−18:42:42
2	00:43:37.6	+00:46:38
3	00:43:45.1	+00:47:53
4	00:43:37.0	+00:48:58
5	00:07:40.6	−00:04:39
6	00:07:44.1	−00:05:40
7	00:59:49.8	−27:36:52

NOTES.– Positions are accurate to $\pm 6''$.

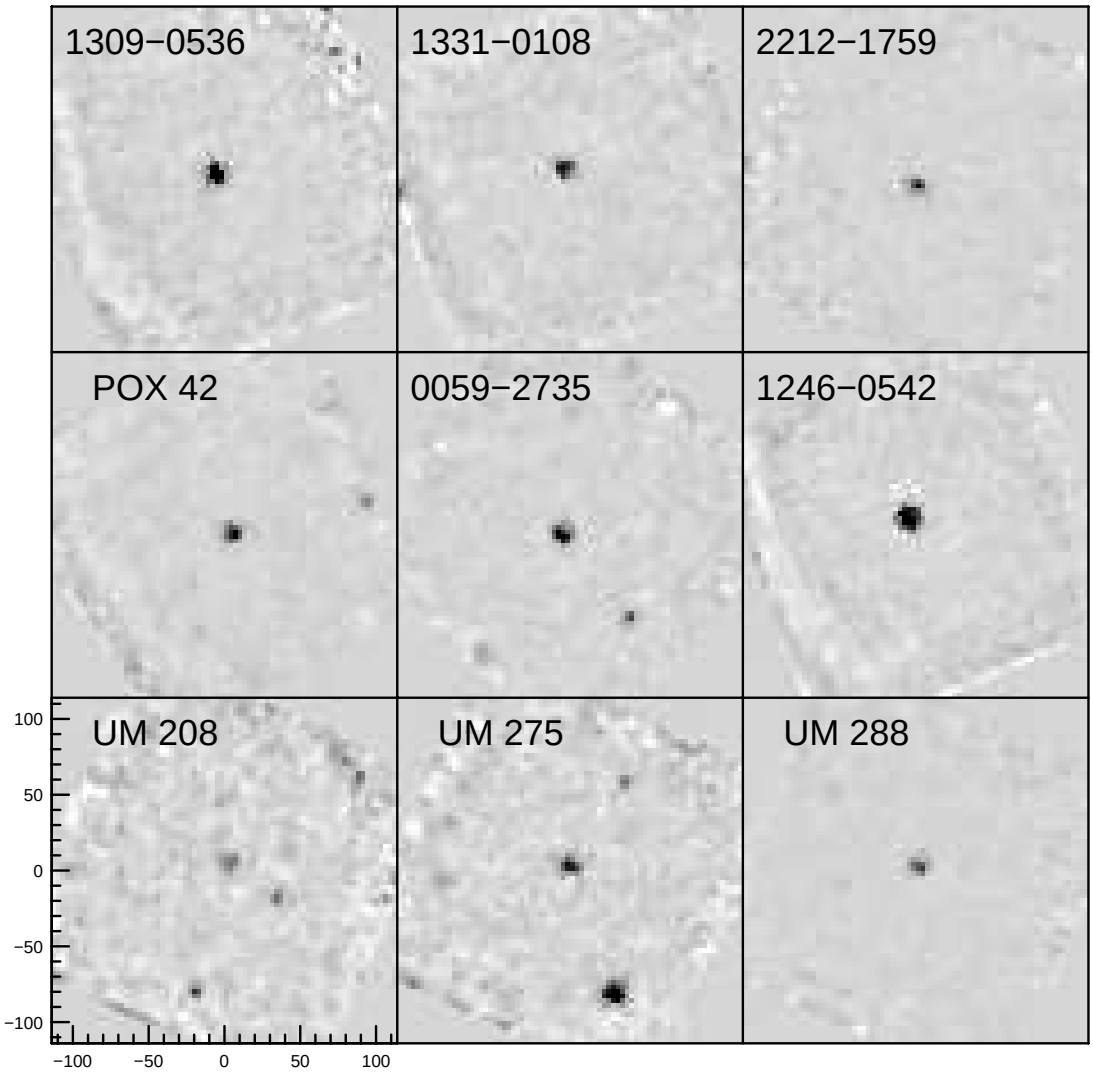

Fig. 1.— 12 μm ISOCAM images of the 9 QSO fields. The central object in each frame is the QSO. North is up and East is to the left.

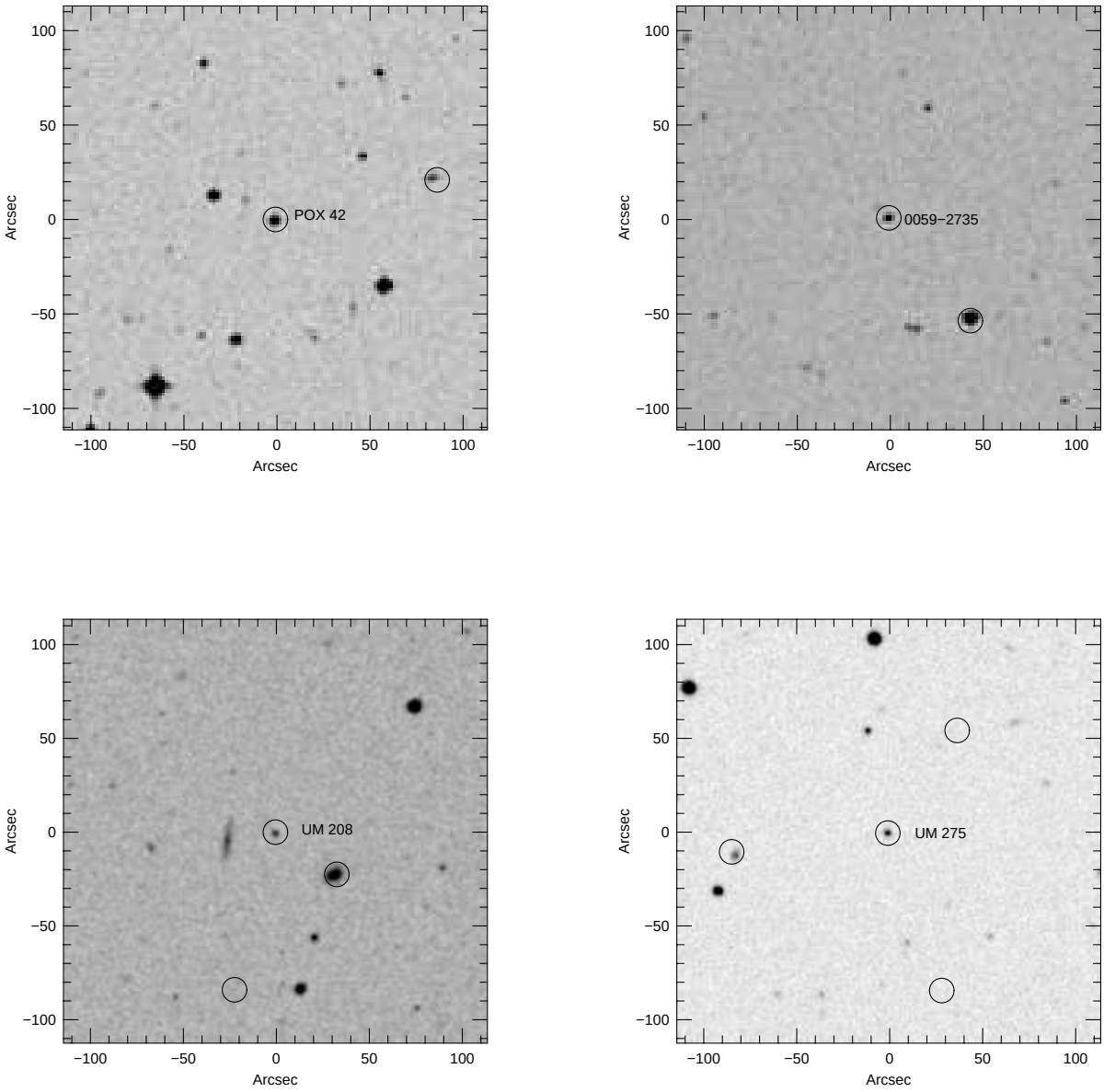

Fig. 2.— Digitized Sky Survey images of QSO fields in which we detected additional sources at 12μm. The central object in all images is the QSO. Circles with a radius of 6$''$ (our 12μm pixel size) are drawn at the locations of objects detected at 12μm.